THE GALAXY ACTIVITY-INTERACTION CONNECTION. II. RADIO OBSERVATIONS

ERIC P. SMITH
Laboratory for Astronomy and Solar Physics, NASA/GSFC, Code 681, Greenbelt, Maryland 20771

NAMIR E. KASSIM
Center for Advanced Space Sensing, Naval Research Laboratory

Received 21 February 1992; revised 18 August 1992

ABSTRACT

As the second part of an ongoing investigation into the triggering of nuclear radio emission in interacting galaxies, we present the results of a Very Large Array snapshot survey of southern interacting galaxies at 6 and 20 cm. The purpose of the survey was to search for and classify the nature of radio emission in a set of advanced-interaction disk galaxies which we had previously imaged optically. There were 42 interacting systems in our sample as well as 10 control systems, none of which had been previously detected by the Parkes surveys. Maps of the radio emission are presented and discussed. The radio properties of the galaxies are compared with their optical and infrared properties to determine the nature of the radio emission. We find that the radio emission in all our interacting galaxies can be attributed to processes associated with a burst of star formation caused by the galaxy interaction. In a specific case (0558−33), we quantitatively confirm earlier models of a starburst, but using radio observations to estimate the number of supernova remnants rather than optical spectra and broadband observations. In no case did we find clear evidence for a buried active nucleus. Further high resolution observations are needed however to better assess the contribution from any compact, weak active nuclei. Despite the obvious interaction these galaxies have undergone, none have developed into powerful radio sources, even though many of the most powerful radio sources are themselves the likely products of galaxy–galaxy interactions. We briefly discuss the implications for the triggering of nuclear activity.

1. INTRODUCTION

1.1 Background

The study of galaxy interactions and their effect on galactic activity has been a productive and busy field for the past decade. In particular, the connection between morphologies of galaxies and/or their interaction state and enhanced radio emission has been well established (e.g., Hummel 1980; Heckman 1983; Hummel *et al.* 1990). We now know that barred galaxies tend to have stronger central radio sources than their nonbarred counterparts, and that galaxies with close (comparable mass) companions or merging galaxies are often even more radio powerful. However, these radio sources are typically several orders of magnitude weaker than the so-called powerful radio sources $\{\log[P_{\rm radio}(\rm W\ Hz^{-1})]\sim 24.5\}$ found in some types of interacting galaxies (Heckman *et al.* 1986). In fact, many of the weaker radio sources in studied interacting galaxies have proven to be of a different nature than those in powerful radio galaxies. While all interacting, powerful radio galaxies have radio sources powered by an active nucleus, most weaker radio sources in interacting systems appear to be dominated by radio emission associated with bursts of star formation with perhaps small contributions from an active nucleus (Hummel *et al.* 1990).

This dichotomy raises the question; if interactions/mergers can trigger the onset of activity in galaxies, as is now widely believed, then why do some interactions result in systems with powerful nuclear activity while others do not? We are attempting to address this question by studying samples of interacting and control galaxies. Having obtained broadband optical images of several of these systems (Smith & Hintzen 1991), we need to establish the level of nuclear activity present. One way of measuring nuclear activity is to search for the presence of nonthermal radio emission. The purpose of our present investigation was to determine the precise levels and nature of radio emission in a sample of "radio weak" interacting systems.

1.2 Sample Selection

Both our interacting and control samples are drawn from the Arp & Madore (1987; hereafter referred to as AM) Catalogue of Southern Peculiar Galaxies and Associations. The interacting sample galaxies were primarily selected based upon their optical morphology as classified by AM and their absence from the Parkes radio survey (flux limit, $S_{2.7\,\rm GHz}\geqslant 0.22$ Jy). We chose to study galaxies AM cataloged as having "tails, loops, or debris" (category 15). There are 291 galaxies in AM with this designation and 86 of these are listed as solely category 15 objects. Many of these 86 systems are no longer two distinct galaxies, but rather single objects with tails or other curvilinear features. In addition to observing objects classified as solely category 15, we imaged galaxies which had multiple category classifications (i.e., in addition to category 15), and a control sample of more widely separated pairs of interacting galaxies. The key feature then of our selection criterion for our "interacting" sample is the presence of a classical optical "tidal" feature.

When choosing this class of object we are explicitly selecting interacting *spiral* galaxies, or interactions involving at least one *disk* system. It has long been known that interacting disk galaxies will produce dramatic tails and loops due to their "cold" dynamical component (Toomre & Toomre 1972). Generally, strong interactions—those that produce significant morphological distortions—are expected when the relative velocity of the encounter is less than the maximum rotational velocity of the galaxy (Binney & Tremaine 1987). Also, since we are interested in studying the manifestations of activity in galaxies, we would expect greater success looking for emission-line signatures in interactions involving spirals because of their greater cool interstellar medium content. The final, yet important, reason for selecting this category of galaxies was their morphological similarity to a subset of powerful radio galaxies, but lack of significant radio emission. This is important because simple arguments based upon the length of the tidal features seen in both types of systems suggest that they have similar interaction ages.

One difficulty associated with any statistical study is the construction of a suitably representative sample of a given population. A second problem is the choice of a control sample. These problems are especially acute in our case because of the complex parameter space provided by galaxy interactions and galactic activity. Having chosen a sample based simply upon the presence of optical tails we are probably selecting interactions involving roughly equal mass participants with relatively slow passages (Toomre & Toomre 1972). Restricting the sample to those objects which have tails *and* distinctly separate nuclei further limits the interactions to those whose ages are less than about $\sim 10^9$ yr (Barnes 1990). We also know that the development of tidal tails, especially the longer ones, requires a few $\times 10^8$ yr, implying that the majority of the galaxies in our sample have interaction ages within a few $\times 10^8$–10^9 yr. It is generally thought that galaxies which are presently interacting come from pairs which were very loosely bound (i.e., may be thought of as having initially parabolic orbits) and are likely to be undergoing their first significant encounter (Toomre & Toomre 1972; Barnes 1990). By selecting galaxies which may be experiencing their first strong encounter, we have chosen an obvious subset of mergers/collisions to examine for the onset of galactic activity. Some of the prices we pay for these selection criteria are that many sample objects will have been interacting for less than 10^9 yr and may not have had the time to exhibit or perhaps even produce the intense nuclear activity found in the most active interacting galaxies, and any activity differences arising from elliptical–elliptical encounters will be missed. Thus, given our selection effects, the question we pose becomes; What are the nature and luminosities of radio sources in a set of advanced mergers involving at least one disk system? As a control sample we have simply chosen, from AM, widely separated spiral galaxies *not* displaying any obvious morphological distortions. These galaxies appear to be natural precursors to the strongly interacting systems.

We note that the majority of the galaxies observed do not have measured redshifts, and hence their absolute radio brightnesses remain unknown. However, unless the systems are phenomenally large, distant interactions, their radio powers are all less than $\log[P_{\rm radio}(\mathrm{W\ Hz^{-1}})] \sim 22.8$ at 20 cm (we assume $H_0 = 75$ km s^{-1} Mpc^{-1} and $q_0 = 0$). Thus, their radio luminosities are well below the break in the radio luminosity function $\{\log[P_{\rm radio}(\mathrm{W\ Hz^{-1}})] \sim 24.5$; Auriemma *et al.* 1977$\}$ which had traditionally been used to separate radio-powerful from mere radio galaxies.

The outline of the paper is as follows. In Sec. 2 we discuss observations and data reduction methods. In Sec. 3 the results for the sample as a whole are presented, along with notes on individual objects. Section 4 contains discussion of the results and plans for future work.

2. OBSERVATIONS

2.1 Very Large Array Observing Setup

Observations towards ~ 50 interacting galaxy candidates south of $\delta = -22°$ were obtained in the *B/C* hybrid configuration of the Very Large Array (VLA) over three consecutive days on 1990 October 5 (9 hr run), October 6 (4 hr run), and October 7 (9 hr run) in two 50 MHz IFs at each of 6 and 20 cm wavelengths using all 27 available antennas. At these wavelengths the bulk of the radio emission from galaxies is nonthermal (Condon & Yin 1990), and therefore suitable for investigations of nuclear "monsters."

Flux density calibration within each band used daily ~ 15 min observations of primary flux density calibrator 3C286, defined to have flux densities of 14.51 and 14.27 Jy at 1.4649 and 1.5149 GHz (20 cm), and 7.41 and 7.46 Jy at 4.8851 and 4.8351 GHz (6 cm), respectively (consistent with the Baars *et al.* 1977 scale). These data were then used to determine the possibly varying flux densities of the secondary (phase) calibrators, which are compact and have well determined positions. CLEANed Contour maps of 6 or 20 cm snapshots images of resolved objects are presented in Fig. 1.

Consecutive 5 min snapshots of nearby secondary calibrators were conducted in both IFs in each band and bracketed observations of pairs of target sources. Target source observations consisted of 2 consecutive 10 min snapshots per source, one each at 6 and 20 cm. Standard computer programs were then used to interpolate the gain and phase of the instrument between calibrator observations. These procedures are normal for the VLA and are thought to provide flux density calibration which is consistent to a few percent with possible systematic errors of up to $\sim 5\%$ at both wavelengths. For a more detailed description of the VLA see Napier *et al.* (1983).

Because of the southern declination of the sources, the range of projected spacings provided in the *B/C* hybrid configuration are comparable to those provided by the VLA in its C array for sources normally observed at higher declinations. The range of available spacings was therefore ~ 0.73–~ 3.4 km, and mean that for these single snapshot observations sources larger than $\sim 3.5'$ at 20 cm or $1'$ at 6 cm may have their flux densities underestimated by

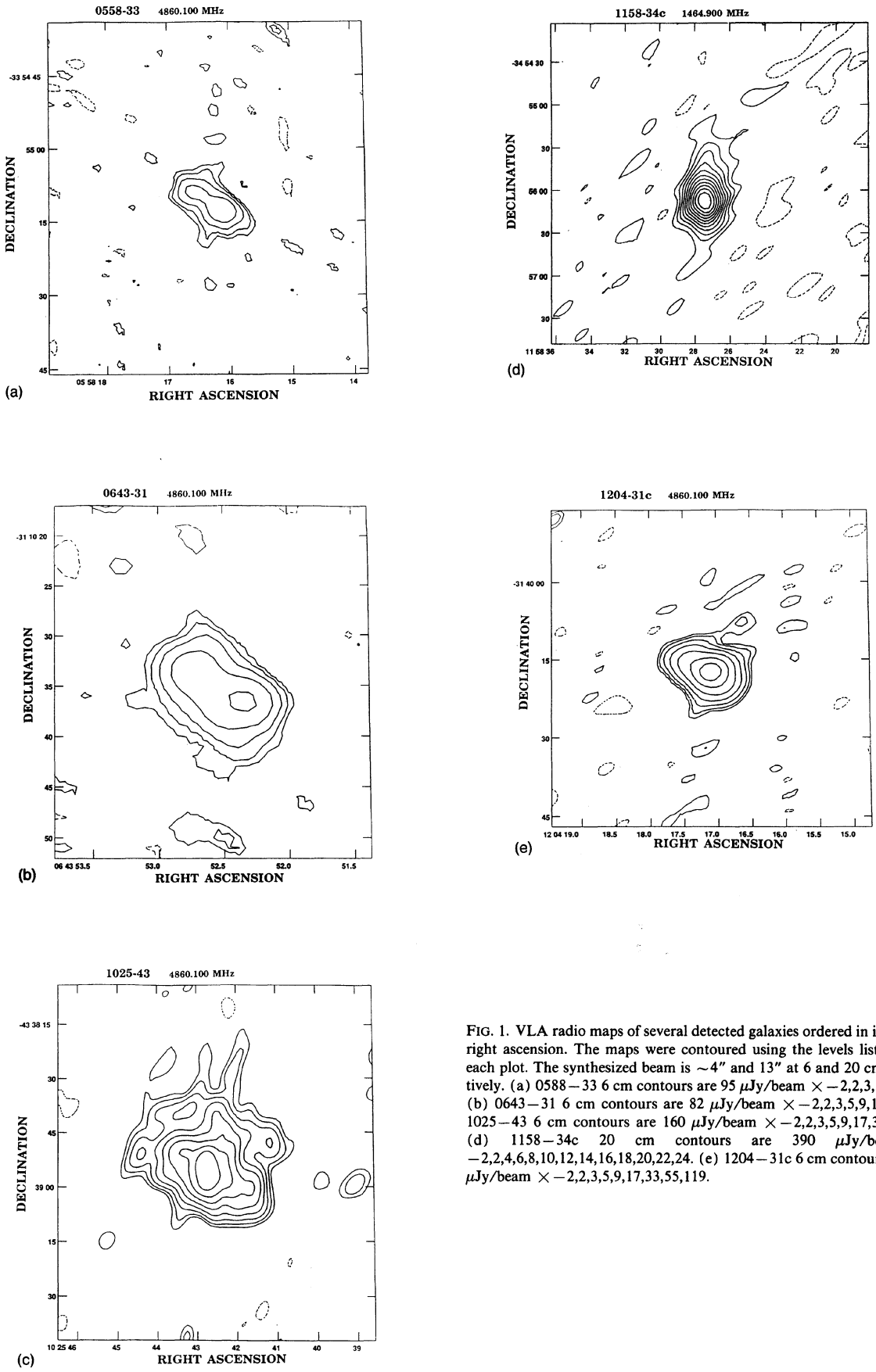

FIG. 1. VLA radio maps of several detected galaxies ordered in increasing right ascension. The maps were contoured using the levels listed below each plot. The synthesized beam is ~4″ and 13″ at 6 and 20 cm, respectively. (a) 0588−33 6 cm contours are 95 μJy/beam × −2,2,3,5,9,17,33. (b) 0643−31 6 cm contours are 82 μJy/beam × −2,2,3,5,9,17,33. (c) 1025−43 6 cm contours are 160 μJy/beam × −2,2,3,5,9,17,33,65,129. (d) 1158−34c 20 cm contours are 390 μJy/beam × −2,2,4,6,8,10,12,14,16,18,20,22,24. (e) 1204−31c 6 cm contours are 113 μJy/beam × −2,2,3,5,9,17,33,55,119.

$\sim 10\%$. None of the sources observed in this study are that extended. The *uv* data from the individual snapshots, after calibration, correction, and inspection for quality were then Fourier transformed to produce "dirty" images which were then CLEANed and restored with elliptical Gaussians. The maps presented in Fig. 1 are all subimages made from these final maps. (No correction for primary beam attenuation was made to the images since all detections were of small-diameter sources near the phase center.) The angular resolution varied from source to source but was typically 4″ at 6 cm and 13″ at 20 cm. The measured rms noise levels near the phase centers were typically ~ 0.13 mJy/beam at 6 cm, and ~ 0.31 mJy/beam at 20 cm.

3. RESULTS

3.1 Entire Sample

We detected 15 out of 42 interacting galaxies and 7 out of 10 control sample galaxies at either 6 or 20 cm. In Table 1 we list the radio positions and measured fluxes (and radio powers when a redshift was available) for the galaxies along with other relevant data. For nondetections we list the $3\sigma_{\rm rms}$ upper limits for the detection of point source. Detection limits for diffuse ($r \gtrsim 4''$ at 6 cm) sources with sizes comparable to the optical sizes in these objects would be on the order of 10–15 times higher. The detected source measurements represent lower limits for the total flux density in cases where there might be extended weak emission. We computed the sample mean spectral index finding, $\langle \alpha \rangle = 0.89 \pm 0.05$ (assuming $S_\nu \propto \nu^{-\alpha}$; see Fig. 2), with no difference between the interacting and control samples. This index is typical for sources whose radio spectrum is dominated by synchrotron emission.

We note that most are of the detected interacting systems are those for which one would naively conclude that the merger is well advanced by the nature of their optical morphology. That is, systems in which the participant galaxies retain their identities are not detected as frequently as systems characterized by a single main luminous body (which may contain distinct nuclei). This is in qualitative agreement with previous studies of interacting galaxies (Balick & Heckman 1982, and references therein).

The radio morphologies of the detected galaxies, with exceptions noted below in Sec. *3.2* or displayed in Fig. 1, were mainly unresolved (5 of 15 detected objects resolved). The radio *morphologies* are consistent with both low level nuclear activity as well as circumnuclear star bursts. However, as we describe in Sec. 4, the latter mechanism appears to be the dominant radio emission producer for most of our objects. We were somewhat surprised by the low detection rate of the interacting sample when compared with the control sample, but attribute this to small sample sizes. Six of the control sample galaxies have published redshifts with a mean $\langle z \rangle = 0.0234$ while the mean of the 8 interacting galaxies with published redshifts is $\langle z \rangle = 0.0184$. The redshifts are similar enough that we are not concerned that the control sample is measuring a much more distant group of objects and hence a brighter population of radio sources (a Malmquist bias).

3.2 Notes on Individual Objects

0558−33: The positions of the two radio and three optical peaks (Smith & Hintzen 1991) are listed in Table 2. The northeast peak in the radio map corresponds to the northeast galaxy optical peak and the southwest radio peak lies within the 3 σ positional error box of the central optical peak. This central optical peak was studied spectroscopically by Olofsson *et al.* (1984) and found to be dominated by a H II regionlike component, with a small shock-heated contribution. We measure the peak flux densities from the northeast and southwest component to be 1.1 and 1.5 mJy, respectively. At the distance of 0558-33 (35 Mpc for $H_0 = 75$) this implies total luminosities greater than 1.6×10^{20} and 2.3×10^{20} W Hz^{-1} at 6 cm. The radio emission associated with the central optical peak is most likely that from electrons accelerated via supernovae remnants generated by a young stellar population. The radio-optical spectral index of this central optical peak $\{R_6 \equiv S_6 \, \mathrm{dex}[0.4(12.5 - B)] = 25\}$ is typical of those found in other interacting/starburst systems (Klein 1982).

If we assume that all stars with $\mathcal{M} \geqslant 8\mathcal{M}_\odot$ are the progenitors of the supernovae which are responsible for the nonthermal radio emission from starbursts (Kennicutt 1984; Condon & Yin 1990) then we can verify whether the radio flux we measure is consistent with the starburst model of Olofsson *et al.* (hereafter referred to as OBE). OBE estimated from their optical spectra that this central region contains a starburst of age $t_{\rm burst} = 1.5 \times 10^7$ yr with a total mass of $2 \times 10^6 \, \mathcal{M}_\odot$.

The radio flux we measure is a combination of thermal and nonthermal components. Condon & Yin (1990) have suggested the ratio of nonthermal to thermal radio emission is roughly constant for spiral galaxies. At our frequency this ratio is ~ 5. To estimate the total nonthermal radio luminosity arising from a population of supernovae we follow Condon & Yin and write:

$$L_{NT}[\mathrm{W\ Hz^{-1}}] \approx 1.3 \times 10^{23} \left(\frac{\nu}{1\mathrm{GHz}} \right)^{-\alpha} \nu_{\rm SN}[\mathrm{yr^{-1}}], \quad (1)$$

where $\nu_{\rm SN}$ is the time averaged supernova rate. Taking the radio flux associated with the central knot as the sum of a thermal and nonthermal part we find $\nu_{\rm SN} \approx 0.005$ yr^{-1}. For the burst age given by OBE, all stars with $\mathcal{M} \geqslant 12.5\mathcal{M}_\odot$ have become supernovae. The total number of supernovae is then just:

$$N_{\rm SN} = \int_{12.5}^{m_u} \Psi(m) dm, \quad (2)$$

where m_u is the upper mass limit of the initial mass function (taken to be $100\mathcal{M}_\odot$), and, $\Psi(m)$ the initial mass function which we assume to be of Salpeter (1955) form, with a slope of $\gamma = 2.35$. Over the assumed age of the burst then we find the averaged supernova rate to be $\nu_{\rm SN} \approx 0.004$ yr^{-1}, consistent with that estimated from the radio flux.

1025−43: This object is the most radio luminous galaxy is our sample, a well-known starburst, and the subject of numerous previous investigations (e.g., Reif *et al.* 1982; Wright *et al.* 1988; Josephs 1991). The 6 cm morphology

TABLE 1. Observed and derived quantities.

OBJECT	R.A. (1950)	dec. (1950)	F_{6cm}	F_{20cm}	α	z	log $[L_{20}$ (WHz^{-1})]	m_V	$q_{4.86\ GHz}$
0029-28	...	...	<0.75	‡	...	...	...	...	...
0030-22	$0^h\ 30^m\ 48.58^s$	-22° 38' 09.0"	5.04	‡	...	...	...	...	2.81
0044-24	...	...	<0.54	‡	...	...	...	...	...
0125-23	...	...	<0.30	<0.75	...	...	...	...	...
0214-23	...	...	<0.30	<0.63	...	...	...	...	...
0240-24	$2^h\ 40^m\ 17.95^s$	-24° 26' 35.0"	1.43	3.20	0.68	...	...	...	...
0242-24	$2^h\ 42^m\ 34.00^s$	-24° 43' 27.0"	0.92	5.40	1.50	...	...	...	2.57
0244-25	...	...	<0.33	<0.60	...	...	...	...	...
0304-25	...	...	<0.30	<0.60	...	...	...	...	...
0318-23	...	...	<0.33	<0.60	...	...	...	...	...
0337-33	...	...	<0.36	<1.32	...	0.0534	<21.4	15.7	...
0541-29	...	...	<2.64	<0.81	...	...	...	...	...
0558-33	see table 2		4.47	11.8	0.82	0.0088	21.3	14.4	2.68
0612-37	...	...	<0.36	<0.75	...	...	...	14.7	...
0643-31	$6^h\ 43^m\ 52.31^s$	-31° 10' 37.0"	4.61	18.1	1.16	...	...	...	2.95
0654-28	$6^h\ 54^m\ 41.87^s$	-28° 17' 21.0"	1.41	4.10	0.90	...	...	14.9	2.97
0839-25c	...	...	<1.50	6.20	...	...	...	...	...
0911-31	...	...	<0.39	<2.13	...	...	...	15.6	...
0926-24	...	...	<0.39	<0.87	...	...	...	16.7	...
0931-25c	...	...	<0.30	<0.63	...	...	...	...	...
0957-27	...	...	<1.50	2.00	...	...	...	...	...
1010-26	...	...	<0.30	<0.81	...	...	...	15.7	...
1015-33c	...	...	<0.30	<0.93	...	0.0090	<20.2	...	...
1018-28c	$10^h\ 18^m\ 04.22^s$	-28° 37' 04.0"	1.12	3.80	1.03	...	...	...	2.77
1024-28	...	...	<0.33	<0.81	...	...	...	...	...
1024-33	...	...	<0.36	<0.75	...	...	...	15.7	...
1025-43	$10^h\ 25^m\ 42.80^s$	-43° 38' 54.0"	240.0	621.0	0.81	0.0094	23.0	11.8	2.61
1028-36	$10^h\ 28^m\ 45.75^s$	-36° 43' 02.0"	18.6	46.3	0.77	...	...	...	...
1112-23	$11^h\ 12^m\ 14.07^s$	-23° 27' 18.0"	24.8	67.3	0.84	0.0120	22.3	13.4	2.74
1112-27	...	...	<0.33	<0.96	...	0.0132	<20.5	14.9	...
1113-27	$11^h\ 13^m\ 04.60^s$	-27° 00' 01.0"	1.80	4.00	0.68	...	...	...	...
1126-34	$11^h\ 26^m\ 48.39^s$	-34° 10' 29.0"	3.78	12.6	1.02	...	...	16.2	2.32
1132-27	...	...	<0.36	<1.06	...	...	...	14.4	...
1146-27	...	...	<0.39	<0.96	...	...	...	14.1	...
1158-34c	$11^h\ 58^m\ 27.50^s$ †	-34° 56' 06.0" †	<1.50	15.4	...	0.0480	22.9	...	...
1204-31c	$12^h\ 04^m\ 17.10^s$	-31° 40' 17.0"	16.6	47.0	0.88	0.0234	22.7	...	2.34
1236-34	$12^h\ 36^m\ 33.45^s$	-34° 31' 14.0"	7.99	29.8	1.11	0.0197	22.4	14.6	...
1254-32	...	...	<0.45	<1.05	...	0.0158	<20.7	13.8	...
1316-24c	$13^h\ 16^m\ 48.15^s$	-24° 13' 19.0"	1.38	4.10	0.92	0.0144	21.2	...	2.94*
1316-24c	$13^h\ 16^m\ 49.24^s$	-24° 13' 41.0"	2.03	4.70	0.71	0.0144	20.0	...	...
1316-28c	...	...	<0.18	<0.81	...	...	...	...	...
1319-25	...	...	<0.39	<4.23	...	...	...	...	...
1320-32	...	...	<0.39	<0.93	...	...	...	14.7	...
1324-37	...	...	<0.45	‡	...	...	...	...	...
1325-25	...	...	<0.42	‡	...	...	...	...	...
1326-23	...	...	<0.54	‡	...	...	...	...	...
1331-23c	$13^h\ 31^m\ 54.42^s$	-23° 11' 27.0"	12.1	36.2	0.93	0.0446	23.2	...	2.02
1332-26	$13^h\ 32^m\ 24.38^s$	-26° 20' 28.0"	4.87	11.5	0.73	...	...	16.3	2.57
1344-30	$13^h\ 44^m\ 33.31^s$	-30° 09' 29.0"	3.92	7.10	0.50	0.0146	21.5	13.3	...
1344-32	...	...	<0.39	<1.14	...	...	...	...	...
1353-25	...	...	<0.33	<0.84	...	...	...	14.7	...
1556-27	...	...	<0.36	<0.81	...	...	...	...	...

Notes to table 1: Column 1 lists the object name, with "c" indicating the control sample objects. Columns 2 and 3 give the 6 cm peak radio positions for galaxies except for (†)1158-34 which lists the 20 cm peak radio positions. Columns 4 and 5 give the observed flux density or 3σ upper limits in mJy at 6 and 20 cm respectively (‡ - indicates no 20cm observation). The spectral index (from $S_\nu \propto \nu^{-\alpha}$) is listed in column 6. The redshift, when known, is listed in column 8, and the log of the radio power at 20cm is listed in column 8 (calculated assuming H_0=75 km s^{-1} Mpc^{-1}). Column 9 gives the visual magnitude from Smith and Hintzen (1991). The parameter $q_{4.86\ GHz}$, a measure of the radio-FIR spectral index at 4.86 GHz, is listed in column 10. (*)Uncertainties in the IRAS positions for 1316-24 prevent a unique idenitfication of the IR source for this object. We have arbitrarily assigned all of the IR flux to the first (1316-24a) source in the table.

of the system is also the most complex in our sample with 4 flux density local maxima within the image, and extensions to the north and south (Fig. 1). The resolved radio morphology, combined with the knowledge that this galaxy is currently undergoing a period of intense star formation implies that the radio emission is probably the result of the supernovae associated with the starburst rather than an indicator of an active nucleus. The spectral energy distribution, from radio through optical, is similar to those of M82 and 0558−33 (Fig. 3).

1158−34c: Two close spirals, one nearly face on and one edge on. The radio peak (Fig. 1) is within the optical image of the southern, edge-on galaxy in this system. The optical peak of this galaxy is located at $\alpha = 11^h\ 58^m\ 27.50^s$, $\delta = -34°\ 56'16''$. We do not detect the northern galaxy ($\alpha = 11^h58^m24.70^s$, $\delta = -34°54'58''$) in this pair at either 6 or 20 cm.

1316−24c: This system is comprised of an elliptical and a nearly edge-on spiral. Neither of the galaxies appear to have grossly distorted or tidal optical morphologies. The radio peaks are approximately spatially coincident with the optical nuclei (see Table 1). We used the HST Guide Star

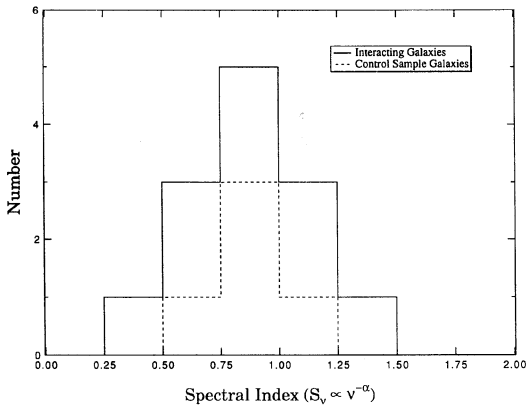

FIG. 2. Distribution of spectral indices α (assuming $S_\nu \propto \nu^{-\alpha}$) for the interacting and control sample galaxies detected at both frequency bands.

catalogue to perform astrometry on the ESO plate to find the optical peak of the elliptical galaxy at $\alpha = 13^h16^m 47.80^s$, $\delta = -24°\ 13'17.8''$, while the optical peak of the edge-on galaxy is at $\alpha = 13^h16^m49.22^s$, $\delta = -24°13'42.8''$.

4. DISCUSSION

4.1 Radio Emission and Galaxy Interactions

Our primary aims were to search for and measure the strength of radio emission in a subset of interacting disk galaxies and a set of control galaxies. Furthermore, we wanted to determine how much of any radio emission was attributable to nuclear activity. The well-known correlation of FIR flux with radio flux (Harwit & Pacini 1975) may be used to discriminate between starburst and active nucleus driven radio emission. The same massive stars which produce the SNRs, and hence the nonthermal radio emission, heat the dust in the galaxy creating this IR-radio correlation. Following Helou *et al.* (1985) we define the parameter q, an FIR-radio spectral index, as

$$q_\nu = \log\left[\frac{\mathrm{FIR}}{3.75\times10^{12}\ \mathrm{Hz}}\right] - \log\left[\frac{S_\nu}{\mathrm{W\ m^{-2}\ Hz^{-1}}}\right],$$

where

$$\left[\frac{\mathrm{FIR}}{\mathrm{W\ m^{-2}}}\right] \equiv 1.26\times10^{-14}\left[\frac{2.58S_{60\,\mu\mathrm{m}} + S_{100\,\mu\mathrm{m}}}{\mathrm{Jy}}\right].$$

The values of q have been determined for a large number of galaxies and been found to be a good discriminator between radio and IR emission powered by starbursts or nuclear activity (Condon *et al.* 1991; Condon & Broderick 1991; Wrobel & Heeschen 1988). The $q_{4.86\,\mathrm{GHz}}$ values for starburst galaxies have small scatters about the mean values of 2.75 (IR selected) or 2.64 (radio selected) and are different from values expected for objects with radio emission primarily powered by nuclear activity ($q_{4.86\,\mathrm{GHz}} \sim 2.2$; Condon & Broderick 1991). The mean $q_{4.86\,\mathrm{GHz}}$ for galaxies (with IR detections) in our survey is 2.65 ± 0.08 suggesting that starbursts are the driving mechanism behind both IR and radio emission. Interestingly, for the two control sample galaxies with *IRAS* point source catalogue listings, we find that $q_{4.86\,\mathrm{GHz}} < 2.3$, similar to that expected for galaxies with active nuclei.

We find no compelling evidence that any of the objects in our interacting sample contains an active nucleus, and perhaps some evidence that two of the objects in the control sample contain weak active nuclei. The bulk of the radio emission from the interacting sample appears to be the result of synchrotron emission from electrons accelerated via SNRs associated with a burst of star formation. Of course, these low-resolution observations do not rule out compact, weak nuclear sources, but it is probable that any such component contains only a minor part of the galaxy energy budget. For those few objects with adequate spectral coverage we note that they have energy distributions similar to classic starburst galaxies. Any nonthermal emission from a nuclear source will likely be less than $\sim 50\%$ of the total radio emission, otherwise it would no longer be dominated by the starburst component. Assuming that our interacting sample radio emission is primarily due to "normal starbursts" then the mean upper limit on the luminosity for any nuclear radio source is on the order of 10^{21} W Hz^{-1}. This limit is consistent with a previous study by Hummel *et al.* (1990) who found compact nuclei of com-

TABLE 2. AM 0558-335 astrometry.

	Feature	R. A. (1950)	Dec. (1950)
Radio	NE lobe	$5^h58^m16.49^s$	$-33°55'9.52'' \pm 0.25''$
	SW lobe	$5^h58^m16.16^s$	$-33°55'12.52''$
Optical	NE galaxy	$5^h58^m16.56^s$	$-33°55'8.6'' \pm 0.7''$
	Center peak	$5^h58^m16.02^s$	$-33°55'13.2''$
	SW galaxy	$5^h58^m15.43^s$	$-33°55'16.1''$

Sky coordinates for the flux peaks in the radio maps and optical images of AM 0558-33.

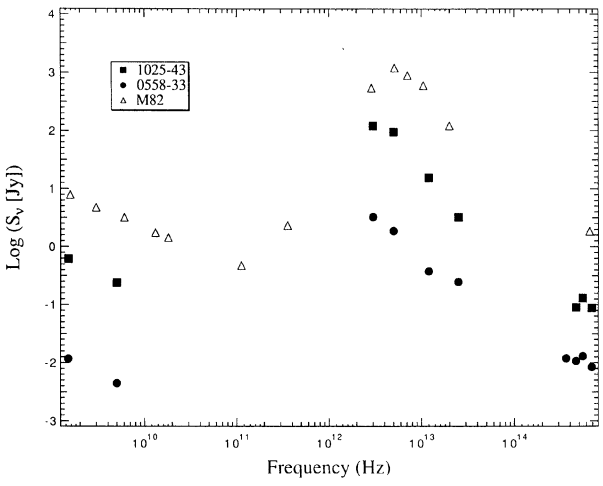

FIG. 3. Spectral energy distributions for two galaxies from the interacting sample plotted along with that of M82, a starbursting galaxy. The downward pointing arrow indicates an upper limit only for the 12 μm passband. Optical data for 0558−33 and 1025−43 and from Smith & Hintzen (1991). Infrared data are from the *IRAS* Point Source Catalog.

parable radio power exist roughly in 20% of interacting spirals.

Even though the interacting sample galaxies must have been experiencing strong tidal deformations for the past few $\times 10^8$ yr none have generated a nuclear monster capable of manifesting itself via strong radio emission often associated with powerful radio galaxies. There are several obvious reasons why stronger nuclear activity might not be present: (a) there may not be a black hole at the center of these galaxies; (b) even if there is a black hole, the fueling process is very inefficient; (c) the energy produced by any activity may be coming out at nonradio frequencies. Current astronomical wisdom would seem to suggest that the latter two possibilities are more likely. If the activity is manifested at other wavelengths however, we still have the question unanswered as to why some interactions produce *radio* galaxies and others do not. Therefore, we posit that perhaps these interacting systems have internal dynamics which have inhibited the production of powerful nuclear radio sources possibly by altering the delivery of material to a central black hole thereby impeding the development of an active nucleus.

4.2 Future Work

The next step in studies of activity triggering in galaxies must begin to address the question of fuel delivery to the nuclear region. While there appears to be little difficulty in getting material into the central few kpc of a galaxy, the transport of this material into its center (fractions of a parsec) remains poorly understood. Further high-resolution radio observations of several of these systems would be profitable. These high resolution data could help place stronger limits on the level of any nuclear component of the emission. Other critical data necessary to extend this work are optical spectra of the interacting systems. With these spectra, another window on the driving processes of their activity would be opened and the kinematics of the interactions may be explored to assess any role they play in the triggering and manifestation of radio activity. Ideally, spectra at several position angles through each system would provide enough information to allow one to distinguish the sense of rotation of each system as well as the relative velocity of the two components. Perhaps there are interaction dynamics which favor the production of strong active nuclei by creating favorable conditions for transporting material into the center of the galaxies. Systems that are highly perturbed (either via retrograde encounters or interactions at high inclination angles) might be better able to deliver fuel to any central black hole than those objects whose central dynamics are undisturbed.

E.S. acknowledges the support of NASA Grant No. 188-451. We thank L. Armus and J. Mazzerella for their assistance in using the *IRAS Faint Source Catalog* and an anonymous referee for his/her many helpful suggestions.

REFERENCES

Arp, H. C., & Madore, B. F. 1987, A Catalog of Southern Peculiar Galaxies and Associations (Cambridge University Press, Cambridge) (AM)
Auriemma, C., Perola, G. C., Ekers, R., Fanti, R., Lari, C., Jaffee, W. J., & Ulrich, M. H. 1977, A&A, 57, 41
Baars, J. W. M., Genzel, R., Pualiny-Toth, I. I. K., & Witzel, A. 1977, A&A, 61, 99
Balick, B., & Heckman, T. M. 1982, ARA&A, 20, 431
Barnes, J. E. 1990, in Dynamics and Interactions of Galaxies, edited by R. Weilen (Springer, Heidelberg), p. 186
Binney, J., & Tremaine, S. 1987, Galactic Dynamics (Princeton University Press, Princeton)
Condon, J. J., & Broderick, J. J. 1991, AJ, 102, 1663
Condon, J. J., Frayer, D. T., & Broderick, J. J. 1991, AJ, 101, 362
Condon, J. J., & Yin, Q. F. 1990, ApJ, 357, 97
Harwit, M., & Pacini, F. 1975, ApJ, 200, L127
Heckman, T. M. 1983, ApJ, 268, 628
Heckman, T. M., et al. 1986, ApJ, 311, 526
Helou, G., Soifer, B. T., & Rowan-Robinson, M. 1985, ApJ, 298, L11
Hummel, E. 1980, A&A, 89, L1
Hummel, E., van der Hulst, J. M., Kennicutt, R. C., & Keel, W. C. 1990, A&A, 236, 333
Josephs, R. D. 1991, in Massive Stars and Starbursts, edited by C. Leitherer, N. R. Walborn, T. M. Heckman, and C. A. Norman (Cambridge University Press: Space Telescope Science Institute, Baltimore), p. 259
Kennicutt, R. C. 1984, ApJ, 277, 361
Klein, U. 1982, A&A, 116, 175
Napier, P. J., Thompson, A. R., & Ekers, R. D. 1983, Proceedings IEEE, 71, 1295
Olofsson, K., Bergvall, N., & Ekman, A. 1984, A&A, 137, 327
Reif, K., Mebold, U., Goss, W. M., van Woerden, H., & Siegman, B. 1982, A&AS, 50, 451
Salpeter, E. E. 1955, ApJ, 121, 161
Smith, E. P., & Hintzen, P. 1991, AJ, 101, 410
Toomre, A., & Toomre, J. 1972, ApJ, 178, 623
Wright, G. S., Josephs, R. D., Roberston, N. A., James, P. A., & Meikle, W. P. S. 1988, MNRAS, 233, 1
Wrobel, J. M., & Heeschen, D. S. 1988, ApJ, 355, 677